



Fermi National Accelerator Laboratory

FERMILAB-Pub-92/222-A

NSF-ITP-92-102

June 1992

Critical behavior in the electroweak phase transition

Marcelo Gleiser

Department of Physics and Astronomy, Dartmouth College, Hanover, NH 03755

Edward W. Kolb

NASA/Fermilab Astrophysics Center

Fermi National Accelerator Laboratory, Batavia, IL 60510

and Department of Astronomy and Astrophysics, Enrico Fermi Institute

The University of Chicago, Chicago, IL 60637

Abstract

We examine the behavior of the standard-model electroweak phase transition in the early Universe. We argue that close to the critical temperature it is possible to estimate the *effective* infrared corrections to the 1-loop potential using well known ε -expansion results from the theory of critical phenomena in 3 spatial dimensions. The theory with the ε -corrected potential exhibits much larger fluctuations in the spatial correlations of the order parameter, considerably weakening the strength of the transition.

PACS numbers: 98.80-k, 98.80.Cq, 12.15.-y

e-mail: gleiser@peterpan.dartmouth.edu; rocky@fnas01.fnal.gov.



I. INTRODUCTION

The possibility that the baryon number of the Universe can be generated at the electroweak phase transition has triggered a lot of interest in understanding the dynamics of weakly first-order phase transitions in the early Universe. Since the original work of Kuzmin, Rubakov, and Shaposhnikov¹ a great deal of effort has been dedicated to the construction of viable models that could generate the required baryon asymmetry.²

As is well-known, one of the necessary ingredients of a successful baryogenesis scenario is a departure from equilibrium. Current scenarios of electroweak baryogenesis rely on the first-order nature of the phase transition to generate the required out-of-equilibrium conditions in the decay of the symmetric metastable phase by the nucleation of bubbles of the broken-symmetric phase. Baryon number is generated by the expansion of the bubble wall either by the scattering of heavy fermions off the wall,³ or by the unwinding of topologically non-trivial configurations in its neighborhood.⁴

Although it is now generally believed that a successful baryogenesis scenario at the electroweak scale requires a departure from the minimal electroweak model, understanding the dynamics of the electroweak phase transition is a crucial ingredient for any viable scenario. One of the main obstacles to a comprehensive study of the electroweak phase transition is our lack of knowledge of the correct effective potential that describes the system in the vicinity of the critical temperature, T_C . Problems due to infrared divergences have been known since the original work of Dolan and Jackiw and Weinberg.⁵ For the current limits on the masses of the Higgs and top quark, the 1-loop effective potential predicts a weak first-order transition.⁶⁻⁸ This is somewhat unsettling, because we know that weak first-order transitions have large infrared divergences which are not accounted for by the 1-loop calculation. In other words, if the 1-loop potential predicts a weak first-order transition, chances are that the actual transition is even weaker, if

not actually second order. It is thus important to incorporate the infrared corrections to the effective potential. In fact, a few recent works have incorporated some infrared corrections caused by the vanishing of vector boson masses near $\phi = 0$ by summing over ring, or daisy, diagrams.⁷ As clearly shown in the paper by Dine *et al.*,⁸ these corrections decrease the effective tunneling barrier for decay, weakening the strength of the transition. The validity of the ring-improved effective potential for the temperatures of interest relies on cutting off higher-order contributions by invoking a non-perturbative magnetic plasma mass, M_{plasma} , for the gauge bosons such that the loop expansion parameter, $g^2 T/M_{\text{plasma}}$, is less than 1. Since this non-perturbative contribution is not well understood at present, one should take the results from the ring-improved potentials with some caution.⁹

In addition to infrared problems caused by the vanishing of the vector boson masses in the symmetric phase, for sufficiently weak transitions we point out that one must take into account infrared divergences caused by the small Higgs mass if $M_H \ll T$. We will review the well-known formalism for field theory at high temperatures. We point out that the loop expansion parameter diverges as the Higgs mass vanishes. This means that diagrams contributing to the 1-loop potential that are unimportant at either high or low temperatures may be dominant around the critical temperature. For instance, at zero temperature the loop expansion parameter for the Higgs loops is λ , the Higgs self coupling. However for the 3-dimensional effective field theory at high temperature, the loop expansion parameter is $\lambda T/M_H(T)$ for the Higgs loops. For $T \gg M_H(T)$, the loop expansion is not under control. We point out that this is exactly the situation in the standard electroweak model between the critical temperature and the spinodal temperature where $M_H(T)$ vanishes.

In this paper, we will attempt to estimate the magnitude of the infrared corrections to the 1-loop electroweak potential near the critical point using a familiar technique from

condensed-matter physics. In particular, we will argue that near the critical point it is possible to estimate the fluctuations in the spatial correlations of the magnitude of the scalar field by using well known results from the theory of critical phenomena. We will show that the effective corrections to the critical exponent that controls the behavior of the correlation length for the electroweak model can be approximated by considering an associated Ginzburg–Landau (G–L) model just above its critical temperature. This approach has been successfully implemented by De Gennes in the study of liquid crystals,¹⁰ and recently by Fernández *et al.* in the study of the two-dimensional 7-states Potts model which exhibits a weak first-order transition.¹¹ In order to make our approach clear it is instructive to examine the critical behavior of the 1-loop effective potential for the electroweak model.

The 1-loop finite-temperature corrections to the electroweak potential have been studied in detail in the literature, most recently by Anderson and Hall.⁶ They showed that a high temperature expansion of the 1-loop potential closely approximates the full 1-loop potential for $M_H \lesssim 150$ GeV and $M_T \lesssim 200$ GeV. (It is important to differentiate between the finite temperature Higgs mass, $M_H(T)$ and the zero-temperature Higgs mass, M_H .) They obtain for the potential

$$V_{\text{EW}}(\phi, T) = D (T^2 - T_2^2) \phi^2 - ET\phi^3 + \frac{1}{4}\lambda_T\phi^4, \quad (1.1)$$

where the constants D and E are given by $D = [6(M_W/\sigma)^2 + 3(M_Z/\sigma)^2 + 6(M_T/\sigma)^2]/24$, and $E = [6(M_W/\sigma)^3 + 3(M_Z/\sigma)^3]/12\pi$. Here T_2 is the temperature at which the origin becomes an inflection point (*i.e.*, below T_2 the symmetric phase is unstable and the field can classically evolve to the asymmetric phase by the mechanism of spinodal decomposition), and is given by

$$T_2 = \sqrt{(M_H^2 - 8B\sigma^2)/4D}, \quad (1.2)$$

where the physical Higgs mass is given in terms of the 1-loop corrected λ as $M_H^2 =$

$(2\lambda + 12B)\sigma^2$, with $B = (6M_W^4 + 3M_Z^4 - 12M_T^4)/64\pi^2\sigma^4$. We use $M_W = 80.6$ GeV, $M_Z = 91.2$ GeV, and $\sigma = 246$ GeV. The temperature-corrected Higgs self-coupling is

$$\lambda_T = \lambda - \frac{1}{16\pi^2} \left[\sum_B g_B \left(\frac{M_B}{\sigma} \right)^4 \ln \left(M_B^2/c_B T^2 \right) - \sum_F g_F \left(\frac{M_F}{\sigma} \right)^4 \ln \left(M_F^2/c_F T^2 \right) \right] \quad (1.3)$$

where the sum is performed over bosons and fermions (in our case only the top quark) with their respective degrees of freedom $g_{B(F)}$, and $\ln c_B = 5.41$ and $\ln c_F = 2.64$.

Apart from T_2 , there will be two temperatures of interest in the study of the phase transition. For high temperatures, the system will be in the symmetric phase with the potential exhibiting only one minimum at $\langle \phi \rangle = 0$. As the Universe expands and cools an inflection point will develop away from the origin at

$$\phi_{\text{inf}} = 3ET_1/2\lambda_T, \quad (1.4)$$

where T_1 is given by

$$T_1 = T_2/\sqrt{1 - 9E^2/8\lambda_T D}. \quad (1.5)$$

For $T < T_1$, the inflection point separates into a local maximum at ϕ_- and a local minimum at ϕ_+ , with $\phi_{\pm} = \{3ET \pm [9E^2T^2 - 8\lambda_T D(T^2 - T_2^2)]^{1/2}\}/2\lambda_T$. At the critical temperature

$$T_C = T_2/\sqrt{1 - E^2/\lambda_T D}, \quad (1.6)$$

the minima have the same free energy, $V_{\text{EW}}(\phi_+, T_C) = V_{\text{EW}}(0, T_C)$. (Note that $V(\phi, T)$ is the homogeneous part of the free energy density whose minima denote the equilibrium states of the system. Accordingly, in this work we freely interchange between calling $V(\phi, T)$ a potential and a free energy density.)

In Fig. 1 we show the electroweak potential at temperatures $T \gg T_1$, T_1 , T_C , T_2 , and $T = 0$. The difference between the temperatures T_1 , T_C , and T_2 is determined by the parameter

$$x = E^2/\lambda_T D. \quad (1.7)$$

This parameter is shown in Fig. 2 for different values of M_H and M_T . Clearly $x \ll 1$ for the minimal electroweak model, so we can write the approximate relations

$$\begin{aligned} T_C &\simeq T_2(1 + x/2) \\ T_1 &\simeq T_2(1 + 9x/16). \end{aligned} \tag{1.8}$$

It is useful to understand why the transition is first order; *i.e.*, why at T_C there is a barrier between the high-temperature phase and the low-temperature phase. It has been appreciated for a long time that a pure $\lambda\phi^4$ theory is equivalent to a Ginzburg–Landau theory, which has a second-order phase transition. The reason the electroweak theory is first order, rather than second order, is that there is an additional attractive force between scalar particles mediated by the vector bosons. This additional attractive force leads to a condensate of the Higgs field at a temperature slightly above T_2 .⁸ T_2 and T_C would be the same (a second-order transition) in the absence of gauge boson interactions. (Note that as $E \rightarrow 0$, *i.e.*, as vector interactions are turned off, $T_C \rightarrow T_2$.)

The whole picture of bubble nucleation relies on the behavior of $V_{\text{EW}}(\phi, T)$ between T_C and T_2 . In the standard picture, one assumes that the system is in a near-homogeneous state around its equilibrium value (in this case $\langle\phi\rangle = 0$), so that large thermal fluctuations in the spatial correlations of ϕ are exponentially suppressed above the scale of the thermal correlation length, $\xi(T)$,

$$\xi^{-2}(T) \equiv M_H^2(T) = \frac{\partial^2 V_{\text{EW}}(\phi = \langle\phi\rangle, T)}{\partial\phi^2}. \tag{1.9}$$

In this case, for some temperature $T_C > T > T_2$, critical bubbles of the broken-symmetric phase appear and expand. They eventually collide with other bubbles, converting the symmetric phase into the broken-symmetric phase.

For the electroweak potential the difference between T_C and T_2 is very small: $\eta_2(T_C) \equiv (T_C - T_2)/(T_C + T_2) \sim x/4 \ll 1$. The transition is predicted to be weakly first order.

As mentioned above, infrared corrections to the 1-loop potential can be very important due to its flatness (small mass) around $\phi = 0$. As we shall see below, the loop expansion parameter for the Higgs loops at high temperatures is not λ , but $\lambda_T T/M_H(T)$. We can estimate where this will become large for the standard electroweak model. Before starting, it is helpful to note that the temperature-corrected Higgs self-coupling, λ_T , is approximately equal to the *tree-level* Higgs self-coupling, $\lambda_0 = M_H^2/2\sigma^2$. (It is easy to see why the temperature-dependent logarithmic correction approximately cancels the zero-temperature 1-loop logarithmic correction if one adopts the renormalization scheme of Ref. 8.) For the electroweak potential near T_C , $M_H^2(T_C) = 2D(T_C^2 - T_2^2)$. Since $T_2^2/T_C^2 = 1 - E^2/\lambda_T D$, $M_H(T_C) = T_C E \sqrt{2/\lambda_T}$. Therefore at T_C the loop expansion parameter is $\lambda_T T_C/M_H(T_C) = \lambda_T^{3/2}/E\sqrt{2}$. Now as discussed above, to a reasonable accuracy $\lambda_T = M_H^2/2\sigma^2$ (here, of course, M_H is the zero-temperature mass). Thus

$$\lambda_T T_C/M_H(T_C) \simeq M_H^3/4E\sigma^3 \sim 1.68(M_H/100 \text{ GeV})^3. \quad (1.10)$$

For M_H greater than about 84 GeV, at T_C the expansion parameter exceeds unity. Between T_C and T_2 the mass goes to zero, so the corrections are even larger.

The question we would like to address in this paper is, can we estimate the magnitude of the infrared corrections in a simple way? Since we are interested in the behavior of the system around $\langle\phi\rangle = 0$ for $T_C \geq T \geq T_2$, we will show that it is possible to map the electroweak potential *in a small neighborhood around $\phi = 0$* to an effective Ginzburg-Landau (G-L) theory which exhibits a second-order phase transition at T_2 . The critical behavior of this model has been extensively studied in the seventies using renormalization group (RG) techniques pioneered by Wilson.¹² In particular, infrared corrections to the G-L model which are important around the critical temperature have been computed using ϵ -expansion techniques. The net result is that the magnitude of fluctuations on the spatial correlations of the order parameter calculated by mean-field theory (which we

will show is equivalent to the 1-loop potential) is largely underestimated. We will obtain the corrections to the G–L model and map it back to the electroweak potential in an attempt to estimate the infrared corrections to the 1-loop result. We will show that the corrections to tunneling rates can be very large, indicating the failure of the naïve 1-loop potential to describe the dynamics of the transition.

This paper is organized as follows. In Section 2 we follow Ginsparg¹³ and show how we can study the finite temperature behavior of a field theory in 4 dimensions ($d = 4$) by looking at the static (zero Matsubara frequency) mode of an effective theory in $d = 3$. We then study the critical behavior of a G–L model in $d = 3$, emphasizing the infrared corrections to the correlation length obtained by ε -expansion methods. In Section 3 we establish the connection between the critical behavior of the electroweak potential and an associated G–L model. We do it using two different G–L models, showing that they give the same results. We obtain an ε -corrected mass and study its effects on the nucleation rate. In Section 4 we strengthen our arguments by estimating the thermal dispersion of the scalar field around the origin and by repeating our recent calculation for the nucleation rate for non-perturbative sub-critical fluctuations. Based on the infrared corrections obtained in Section 3, we argue that sub-critical bubbles offer a simple estimate of the failure of the 1-loop result. We end in Section 5 with general comments on the nature of weak first-order transitions.

II. CRITICAL BEHAVIOR OF ϕ^4 FIELD THEORY

In order to study the critical behavior of a ϕ^4 scalar field theory we follow Ginsparg¹³ in reducing the theory to an effective theory of the static mode of the scalar field in $d = 3$ dimensions. The generating functional in the presence of a source $J(x)$ for a zero

temperature scalar field theory in Euclidean ($t = -i\tau$) space-time is (we use $\hbar = c = 1$)

$$Z[J] = \int [\mathcal{D}\phi] \exp \left\{ - \int d^4x \left[\frac{1}{2} (\partial\phi)^2 - \frac{1}{2} m^2 \phi^2 + \frac{\lambda}{4} \phi^4 \right] - \int d^4x J\phi \right\}. \quad (2.1)$$

In order to study the theory at finite temperature we take the Euclidean time to be periodic in β , and sum only over periodic paths with $\phi(0, \mathbf{x}) = \phi(\tau, \mathbf{x})$, as is well known.⁵

Due to the periodic behavior in τ we can expand the scalar field as

$$\phi(\tau, \mathbf{x}) = \frac{1}{\beta} \sum_{n=-\infty}^{+\infty} \int \frac{d^3\mathbf{k}}{(2\pi)^3} \exp(i\omega_n \tau + i\mathbf{k} \cdot \mathbf{x}) \phi_n(\mathbf{k}); \quad \omega_n = 2\pi n/\beta. \quad (2.2)$$

By rescaling the field $\phi_n(\mathbf{k})$ by $\beta^{-1/2}$, and separating the static ($n = 0$) mode from the rest, we obtain,

$$\begin{aligned} Z[J] = & \int_{\text{periodic}} [\mathcal{D}\phi] \exp \left\{ - \int_{\mathbf{k}} \frac{1}{2} (\mathbf{k}^2 - m^2) \phi_0(\mathbf{k}) \phi_0(-\mathbf{k}) \right. \\ & - \sum_{n \neq 0} \int_{\mathbf{k}} \frac{1}{2} [(2\pi n/\beta)^2 + \mathbf{k}^2 - m^2] \phi_n(\mathbf{k}) \phi_{-n}(-\mathbf{k}) + \int J\phi \\ & \left. - \frac{\lambda/\beta}{4} \sum_{n, n', n''=-\infty}^{+\infty} \int_{\mathbf{k}, \mathbf{k}', \mathbf{k}''} \phi_n(\mathbf{k}) \phi_{n'}(\mathbf{k}') \phi_{n''}(\mathbf{k}'') \phi_{-n-n'-n''}(-\mathbf{k} - \mathbf{k}' - \mathbf{k}'') \right\} \end{aligned} \quad (2.3)$$

where $\int_{\mathbf{k}} = \int d^3\mathbf{k}/(2\pi)^3$. The effective $d = 3$ theory is obtained by summing over all the $n \neq 0$ modes. Perturbatively, this means that all internal lines in the Feynman diagrams will correspond to sums over the $n \neq 0$ modes, and the external lines are given only by the $n = 0$ mode. This way the higher modes will contribute to the mass, wave-function renormalizations, and to the N -point function for the effective theory of the $n = 0$ mode. It is then possible to construct an effective Lagrangian \mathcal{L}_{eff} for the $d = 3$ theory by a systematic perturbation expansion in λ . The leading contribution to the 2-point function is given by the tadpole diagram obtained by summing over the higher modes in the Feynman propagator. One obtains to leading order,

$$\mathcal{L}_{\text{eff}} = \frac{1}{2} \left(-m^2 + \frac{\lambda}{4\beta^2} + \dots \right) \phi_0(\mathbf{k}) \phi_0(-\mathbf{k}) + \frac{\lambda/\beta}{4} \phi_0^4 + \dots \quad (2.4)$$

Note that in the effective $d = 3$ theory the coupling λ is dimensionful with the temperature naturally setting its dimensionality. This temperature dependence will not be

relevant for the discussion of the critical behavior of the theory and will be absorbed into the definition of λ . The static critical behavior of the original $d = 4$ theory is completely embodied in the effective theory for the $n = 0$ mode in $d = 3$. To leading order in λ , this theory exhibits a phase transition at a critical temperature

$$T_C^2 = 1/\beta_C^2 = \frac{4m^2}{\lambda} (1 + O(\lambda) + \dots). \quad (2.5)$$

It turns out that the critical behavior of the theory above, known as the G-L model, has been extensively studied using the ε -expansion to incorporate higher-order infrared effects. From \mathcal{L}_{eff} we can obtain the effective 3-dimensional potential to leading order in λ ,

$$V_{\text{G-L}}(\phi, T) = \frac{m^2(T)}{2} \phi^2 + \frac{\lambda}{4} \phi^4; \quad m^2(T) \equiv \frac{\lambda}{4} (T^2 - T_C^2), \quad (2.6)$$

where $\phi(\mathbf{x})$ is the static scalar field, which is the relevant order parameter in equilibrium.

As is well-known,¹⁴ this theory exhibits a second-order phase transition at T_C ; above T_C the left-right symmetry is exact and the equilibrium value of ϕ is $\langle \phi \rangle = 0$. Below T_C the symmetry is broken and the equilibrium value of ϕ is $\langle \phi \rangle = \pm [m^2(T)/\lambda]^{1/2}$. In the thermodynamic limit, the system will eventually settle at one value of ϕ , since any interface is energetically unfavored. Of course $\langle \phi \rangle$ only gives information about the homogeneous behavior of ϕ . Typically, there will be fluctuations around $\langle \phi \rangle$ which are correlated within the correlation length scale defined in Eq. (1.9). For temperatures above and below T_C (denoted by $+$ and $-$ respectively) we obtain from Eq. (2.6)

$$\xi_+^{-2}(T) = m^2(T) = \frac{\lambda}{4} T_C^2 (1 + T/T_C)^2 \left(\frac{T - T_C}{T + T_C} \right), \quad (2.7)$$

and

$$\xi_-^{-2}(T) = -2m^2(T) = \frac{\lambda}{2} T_C^2 (1 + T/T_C)^2 \left(\frac{|T - T_C|}{T + T_C} \right). \quad (2.8)$$

This is the well known result from mean-field theory, usually expressed as

$$\xi_{\text{MF}}(T) \propto |T - T_C|^{-\nu}; \quad \nu = 1/2, \quad (2.9)$$

where the critical exponent ν expresses the singular behavior of $\xi(T)$ as $T \rightarrow T_C$ both from above and below. In Fig. 3 we show the results for a dynamical simulation of a $d = 2$ G-L model for various values of T .¹⁵ It is clear from this simulation that fluctuations around the equilibrium value of ϕ are indeed very large near T_C , being considerably larger than the mean field results. Thus, the assumption of near homogeneity is not valid if T is sufficiently close to T_C .

In order to handle the infrared divergences that appear near T_C , the RG is used to relate a given theory to an equivalent theory with larger masses and thus better behaved in the infrared. Within the ϵ expansion, one works in $4 - \epsilon$ dimensions and finds a fixed point of order ϵ of the RG equations, taking the limit $\epsilon \rightarrow 1$ in the end. We refer the interested reader to Ref. 14 for details. To second-order in ϵ one obtains,

$$\nu = \frac{1}{2} + \frac{1}{12}\epsilon + \frac{7}{162}\epsilon^2 \simeq 0.63. \quad (2.10)$$

The corrected critical exponent embodies corrections coming from the infrared divergences near T_C . The ϵ -corrected correlation length can be written above T_C as

$$[\xi_+^\epsilon(T)]^{-1} = \sqrt{\frac{\lambda}{4}} T_C (1 + T/T_C) \left(\frac{T - T_C}{T + T_C} \right)^{0.63}. \quad (2.11)$$

Below T_C we obtain,

$$[\xi_-^\epsilon(T)]^{-1} = \sqrt{\frac{\lambda}{2}} T_C (1 + T/T_C) \left(\frac{|T - T_C|}{T + T_C} \right)^{0.63}, \quad (2.12)$$

so that, in both cases the ratio between the mean field and ϵ -corrected correlation lengths can be written as

$$\frac{\xi_{\text{MF}}(T)}{\xi_\epsilon(T)} = \eta_C^{0.13}(T); \quad \eta_C(T) \equiv \frac{|T - T_C|}{T + T_C}. \quad (2.13)$$

If we are interested in studying the behavior of the theory above T_C we can use the fact that $\xi(T) = m^{-1}(T)$ to obtain an ε -corrected mass,

$$m_\varepsilon(T) = \eta_C^{0.13}(T)m(T). \quad (2.14)$$

A similar result can be easily obtained below T_C .

III. INFRARED CORRECTIONS TO THE ELECTROWEAK POTENTIAL

In this section we will argue that we can obtain information on the critical behavior of the electroweak phase transition between T_C and T_2 by studying a G–L model with a critical temperature that we take to be T_2 . This is possible since T_C is so close to T_2 due to the weakness of the transition already at 1-loop level. [See Fig. 2.] Thus, we will estimate the infrared corrections to the electroweak model by looking at the G–L model around T_C . Clearly this is only an approximation to treating the full problem of incorporating the ε -expansion for the standard model. However, from the nature of the potential, we claim that our results are a lower bound on the true infrared corrections, which we conjecture will be even more severe than what we will estimate below.

3.1 MATCHING TO A G–L MODEL ABOVE ITS CRITICAL TEMPERATURE

We start with the simplest possible approach, by studying the G–L model defined by the free energy density,

$$V_{\text{G-L}}(\phi, T) = \frac{m^2(T)}{2}\phi^2 + \frac{\lambda_T}{4}\phi^4; \quad m^2(T) \equiv 2D(T^2 - T_2^2), \quad (3.1)$$

where D , T_2 , and λ_T are defined in the Introduction. This is simply $V_{\text{EW}}(\phi, T)$ with $E \rightarrow 0$. This model exhibits a second-order phase transition at $T = T_2$. Recall that this

is the temperature at which the barrier disappears in the 1-loop electroweak potential. [See Fig. 1.] Thus, we are interested in the behavior of this model for temperatures above T_2 . The claim is that for $T \lesssim T_C$ and in the neighborhood of $\langle\phi\rangle = 0$ this model can be used to give us an *estimate* of the infrared corrections to the electroweak potential. Note that our choice of the mass is such that the correlation length for fluctuations around equilibrium is the same in both models. In Fig. 4 we compare the electroweak potential and the G–L model discussed above for $T = T_C$ and $T = T_2$. Note how the behavior around $\langle\phi\rangle = 0$ is well-matched by the G–L model

From the results of the previous section, the ε -corrected mass is

$$m_\varepsilon^2(T) = 2D\eta_2^{0.26}(T) (T^2 - T_2^2); \quad \eta_2(T) = \frac{|T - T_2|}{T + T_2}. \quad (3.2)$$

The value of $\eta_2(T)$ at $T = T_C$ can be found using T_C and T_2 from Eqs. (1.6) and (1.2):

$$\eta_2(T_C) = \frac{1 - \sqrt{1 - E^2/\lambda_T D}}{1 + \sqrt{1 - E^2/\lambda_T D}}. \quad (3.3)$$

In Fig. 5 we show $m_\varepsilon^2(T_C)/m^2(T_C) = \eta_2^{0.26}(T_C)$ as a function of the Higgs mass for several values of the top mass. It is clear that the infrared corrections are quite large for all values of parameters probed. Below T_C the potential is even flatter near the origin and the infrared problem is even more severe. For larger values of ϕ the cubic term becomes important increasing the flatness of the electroweak model compared to the G–L model (leading again to more severe infrared problems). Before we go on to discuss possible implications of the ε -corrections to the electroweak phase transition we study the same problem with a different G–L model next.

3.2 MATCHING WITH G-L IN THE PRESENCE OF EXTERNAL FIELD

Information about the critical behavior of the electroweak transition by studying a simpler system can be obtained introducing a new field such that the electroweak potential (neglecting the left-right symmetry!) becomes equivalent to a G-L model with an external field which is temperature dependent. In other words, we can transform away the cubic term in $V_{EW}(\phi, T)$ by defining

$$\phi' = \phi - ET/\lambda_T, \quad (3.4)$$

such that

$$V'(\phi', T) = AT(T^2 - T_C^2)\phi' + B(T^2 - T_C^2)\phi'^2 + \frac{\lambda_T}{4}\phi'^4 + \dots \quad (3.5)$$

where \dots represents terms independent of ϕ' and

$$A = \frac{2ED}{\lambda_T} (1 - E^2/\lambda_T D); \quad B = D (1 - 3E^2/\lambda_T D). \quad (3.6)$$

The temperature T_C' appearing in Eq. (3.5) is given by

$$T_C'^2 = \frac{T_2^2}{1 - 3E^2/2\lambda_T D} \sim T_2^2(1 + 3x/2). \quad (3.7)$$

The potential $V'(\phi', T)$ is shown in Fig. 6 for several values of the temperature. The coefficient of the linear term can be interpreted as a temperature-dependent external field which vanishes at T_C . At T_C the potential has a double-well shape, so that below T_C the minimum at ϕ'_- becomes metastable, while the barrier separating ϕ'_- from the global minimum at ϕ'_+ disappears at T_2 . Also, one can see that the location of the minimum at ϕ'_- is roughly temperature independent. Hence, the system exhibits the same critical behavior around ϕ'_- as the electroweak model around $\phi = 0$. We can see this by evaluating

$$m_-^2(T) = \frac{\partial^2 V'(\langle \phi \rangle = \phi'_-, T)}{\partial \phi'^2} = 2B(T^2 - T_C'^2) + 3\lambda_T \phi_-'^2. \quad (3.8)$$

Using that at T_C the potential is a double-well and that ϕ'_- is roughly temperature independent, we find that

$$\phi'_- \simeq - \left[\frac{2B(T_C'^2 - T_C^2)}{\lambda_T} \right]^{1/2}. \quad (3.9)$$

Since $E^2/\lambda_T D \ll 1$ for all values of the Higgs and top masses we consider, we can write

$$m_-^2(T) \simeq 2D (T^2 - T_2^2) \left(1 - \frac{3}{2} E^2/\lambda_T D \right) \simeq m^2(T), \quad (3.10)$$

where $m^2(T)$ is defined in Eq. (3.1). Since we have shown that $m_-^2(T) \simeq m^2(T)$, it is legitimate, within our framework, to use the results from the ε -expansion for the G-L model of ϕ' directly into the electroweak model for $T \lesssim T_C$ and in the neighborhood of $\phi = 0$. As the relevant critical temperature of this G-L model is also T_2 , the results are identical to those of Eq. (3.2).

Again we stress that this is not intended to be an exact calculation of the infrared corrections to the electroweak potential, but simply an estimate of the magnitude of these corrections for small ϕ . As mentioned earlier, we expect the true corrections to be even more severe than what we obtained above.

As a possible application of the above results, we estimate the corrections to the 1-loop tunneling rate using $m_\varepsilon^2(T)$. This is clearly an approximation since we have stressed that our approach is only valid in a small neighborhood of $\langle \phi \rangle = 0$, and should not be trusted for $\phi \gtrsim D(T^2 - T_2^2)/ET$, for a given T . We want to estimate how severe the corrections to tunneling could be due to the smallness of the curvature at the origin. The finite-temperature tunneling rate, $\Gamma \propto \exp(-S_3/T)$, for a theory with a potential like the electroweak potential has been shown by Dine *et al.*⁸ to have an approximate analytical expression for the exponent given by

$$\frac{S_3}{T} = 4.85 \frac{m^3(T)}{E^2 T^3} f(\alpha) \quad \alpha = \frac{\lambda_T m^2(T)}{2E^2 T^2}, \quad (3.11)$$

with

$$f(\alpha) = 1 + \frac{\alpha}{4} \left[1 + \frac{2.4}{1-\alpha} + \frac{0.26}{(1-\alpha)^2} \right]. \quad (3.12)$$

However, according to our arguments, for $T < T_C$ the effective curvature of the potential around the equilibrium point is smaller than what is estimated from the 1-loop approximation. The effective tunneling barrier is then also smaller, and the kinetics of the transition may be different from the usual nucleation scenario. [An interesting possibility is that the critical temperature for the corrected theory is larger than the 1-loop result. This is also true for the results of Refs. 7 and 8, where the cubic term is weakened due to the infrared corrections coming from the gauge bosons. However, as we remarked earlier, our method is only applicable in a small neighborhood of ϕ , and we cannot use it to study the potential away from the origin which is necessary to predict T_C in a first order phase transition. We are presently investigating this question.] Taking into account the ε -corrections above, the exponent becomes,

$$\frac{S_3^\varepsilon}{T} = 4.85\eta_2^{0.39}(T) \frac{m^3(T)}{E^2 T^3} f(\alpha_\varepsilon); \quad \alpha_\varepsilon = \eta_2^{0.26}(T) \frac{\lambda_T m^2(T)}{2E^2 T^2}. \quad (3.13)$$

Clearly use of the ε -expansion improved mass can have an enormous effect upon the tunnelling rate, changing the *exponent* by a large factor.

IV. THERMAL FLUCTUATIONS AND SUB-CRITICAL BUBBLES

In this section we discuss how it is possible to examine the strength of a first-order transition by two simple methods. The first method, introduced by one of us,¹⁶ relies on estimating the magnitude of the thermal dispersion of the order parameter around its equilibrium value. The second method based on the work of Gleiser, Kolb and Watkins,¹⁷ relies on estimating the thermal nucleation rate of “sub-critical bubbles,” which are

correlation volume fluctuations of one phase inside the other phase. We will argue that when applied to the electroweak phase transition, both methods give results which are qualitatively consistent with each other, signaling the failure of the naïve 1-loop potential as a valid approximation to study the dynamics of the transition.

4.1 THERMAL DISPERSION AROUND EQUILIBRIUM

Consider a system described by some potential which at a given temperature T exhibits at least a local minimum at some value of the local order parameter, $\phi = \langle \phi \rangle$. For example, the electroweak potential of Fig. 1 has a global (and, below T_C local) minimum at $\langle \phi \rangle = 0$ for all $T > T_2$. If we are interested in studying nucleation below T_C , we should require that the system is in a near homogeneous phase characterized by $\langle \phi \rangle = 0$. That is, although there will be fluctuations around equilibrium, they should be small enough so that when calculating the transition rate the usual boundary conditions at infinity apply. However, from our previous discussion, for weakly first-order transitions infrared corrections can be important, and large fluctuations around equilibrium are to be expected for temperatures below T_C . It is then legitimate to ask if the usual assumption of near-homogeneity is valid. In Ref. 16 a simple method was introduced in order to answer qualitatively this question. Using a Gaussian approximation to the potential, we compare the thermal dispersion of the order parameter around its equilibrium value for a certain length scale $r = |x - y|$, denoted by $\langle \phi(x)\phi(y) \rangle_\beta$, to the value of the order parameter at the inflection point of the potential, denoted by ϕ_{inf} . Simple physical arguments show that the relevant length scale is the correlation length, ξ .¹⁶ If the magnitude of the thermal dispersion is comparable to the value of ϕ at the inflection point, the system has a large probability to overcome the barrier thermally, populating other accessible

minima. In equations, if we have

$$\sqrt{\langle \phi(0)\phi(\xi) \rangle_\beta} \lesssim |\phi_{\text{inf}} - \langle \phi \rangle|, \quad (4.1)$$

the assumption of near-homogeneity is probably incorrect. In Ref. 16 this condition was applied to the top of the barrier instead of the inflection point. That gives a very conservative estimate, since at the top of the barrier non-linearities are obviously important, enhancing the magnitude of the thermal dispersion. Strictly speaking, the Gaussian approximation is only valid up to the inflection point.

In a recent work, Tetradis applied the above method to the electroweak transition showing that indeed the probability of fluctuations over the barrier is large.¹⁸ He used an approximate expression for calculating $\langle \phi^2 \rangle_\beta$ given in Ref. 16. Here we would like to compute the thermal dispersion in more detail, and again apply the results to the electroweak transition. We will show that the dispersion is still quite large, in qualitative agreement with our previous results based on the ε -expansion.

For a free massive scalar field theory in thermodynamic equilibrium at temperature T , the two-point function can be written in terms of a zero temperature part and a finite temperature part after time ordering as¹⁹

$$\begin{aligned} \langle \hat{T} \phi(x)\phi(y) \rangle &= i \int \frac{d^4k}{(2\pi)^4} \frac{e^{-ik(x-y)}}{k^2 - m^2 + i\varepsilon} \\ &+ \int \frac{d^3k}{(2\pi)^3 2\omega_k} \frac{1}{e^{\beta\omega_k} - 1} \left(e^{-ik(x-y)} + e^{ik(x-y)} \right), \end{aligned} \quad (4.2)$$

where $\omega_k^2 = k^2 + m^2$.

Here we will focus on the temperature dependent part only. In spherical coordinates we can write

$$\langle \phi(0)\phi(|\mathbf{r}|) \rangle_\beta \equiv \Delta(|\mathbf{r}|, \beta) = \int \frac{d|\mathbf{k}||\mathbf{k}^2|}{(2\pi)^2 \omega_k} \frac{\cos(|\mathbf{k}||\mathbf{r}|\cos\theta) \sin\theta d\theta}{e^{\beta\omega_k} - 1}. \quad (4.3)$$

Using properties of Bessel functions $\Delta(\mathbf{r}, \beta)$ can be written as [for details see Ref. (20)],

$$\Delta(|\mathbf{r}|, \beta) = \frac{m}{2\pi^2} \sum_{n=1}^{\infty} \frac{K_1 \left[m\beta \sqrt{n^2 + (|\mathbf{r}|/\beta)^2} \right]}{\sqrt{n^2 + (|\mathbf{r}|/\beta)^2}}, \quad (4.4)$$

where $K_1[z]$ is the modified Bessel function of first kind. From the asymptotic properties of Bessel functions one obtains, in the high temperature limit,

$$\Delta(0, m\beta \ll 1) \simeq \frac{T^2}{12}, \quad (4.5)$$

where we used that $\beta = T^{-1}$. We are interested in fluctuations of a correlation volume at a temperature T . In the spirit of the Gaussian approximation we will take the mass m in the above formula to be the curvature of the potential around its equilibrium point at a temperature T , as defined in Eq. (1.9). [This is precisely what is done in the traditional analysis of fluctuations in a Ginzburg–Landau model.²¹] The correlation length is then simply $\xi = m^{-1}$ and we can write

$$\Delta(\xi(T), T) = \frac{T^2}{2\pi^2} \sum_{n=1}^{\infty} \frac{x}{\sqrt{n^2 + x^{-2}}} K_1 \left[x \sqrt{n^2 + x^{-2}} \right]; \quad x \equiv m/T. \quad (4.6)$$

The probability that a fluctuation of correlation volume around equilibrium can “spread” over the inflection point is then simply,

$$P(\langle \phi \rangle \rightarrow \phi_{\text{inf}}) \sim \exp \left[-\frac{(\langle \phi \rangle - \phi_{\text{inf}})^2}{2\Delta(\xi(T), T)} \right], \quad (4.7)$$

where it should be clear that $\langle \phi \rangle$ and ϕ_{inf} are in general temperature dependent quantities. It is straightforward to apply this formula to the electroweak transition at T_C . $m^2(T)$ is given in Eq. (3.1) and ϕ_{inf} for $T \leq T_1$ is given by

$$\phi_{\text{inf}} = \frac{ET}{\lambda_T} \left[1 - \sqrt{1 - \frac{2D\lambda_T}{3E^2} (1 - T_2^2/T^2)} \right]. \quad (4.8)$$

The results are shown in Fig. 7 as a function of the Higgs mass for $M_T = 130$ GeV. It is clear that thermal fluctuations are quite large at T_C , in agreement with our previous

results. Since the 1-loop potential is evaluated for small fluctuations around the equilibrium value, this simple criterion indicates that the 1-loop approximation to the effective potential is not reliable around T_C .

4.2 SUB-CRITICAL BUBBLES

We now discuss another criterion to estimate the validity of the 1-loop approximation to the effective potential, based on the “sub-critical bubbles method” discussed in Ref. 17. Since we have recently applied this method to the electroweak potential of Eq. (1.1), we will be quite brief here and refer the reader to Ref. 22 for details.

Consider the electroweak potential of Fig. 1. Below T_1 a new minimum develops at ϕ_+ away from the symmetric minimum at $\langle\phi\rangle = 0$. There will be a non-zero probability for bubbles of radius R of the new phase at ϕ_+ to be thermally nucleated. The thermal nucleation rate for producing a bubble of radius R is given by $\Gamma(R, T) \sim \exp[-F(R)/T]$, where $F(R)$ is the free energy of the fluctuating region of radius R . For $T \geq T_C$ it is clear that the larger the bubble the more unfavored it is, since the free energy is a monotonically increasing function of R . The bubbles will shrink in a time scale determined by many factors. For example, for a curvature dominated motion of the bubble wall, which is probably a good approximation close to T_C , the radius of a large bubble shrinks as $t^{1/3}$.²³ Some recent numerical studies showed that even small bubbles persist longer than one would naïvely estimate, bouncing back a few times before dissipating all their energy into quanta of the field.²⁴ However, due to the exponential suppression in their production rate, unless the transition is very weakly first order (with the whole bubble picture being invalid in this case), only bubbles with small enough radius can be efficiently produced so that at any given time a reasonable fraction of the Horizon volume can be occupied by the new phase at ϕ_+ . Although there is a distribution of bubbles with different radii, it is clear

from the above arguments that bubbles with a correlation volume will be statistically dominant. [The kinetics of the transition is bound to be much more complicated than these simple arguments may imply. There will be many different processes contributing to the number density of bubbles of a given radius as a function of time, such as capture and evaporation of particles from bubbles, coalescence due to bubble collisions, shrinking of larger bubbles, neighbor-induced nucleation, and possible shape instabilities, to name just a few.²⁵ A quick glance at Fig. 3 should convince the reader of this.]

The basic idea behind the sub-critical bubbles method is that for sufficiently weak first order transitions, the rate for producing bubbles of a correlation volume is quite large, so that at any given time there will be an appreciable fraction of the total volume occupied by the new phase. If this is the case, the usual assumption of near-homogeneity used in vacuum decay calculations is not valid; instead of having critical bubbles being nucleated on a background of the metastable phase, nucleation would occur in a background which is better described by a dilute gas of small, non-perturbative fluctuations. There is no reason to expect that the usual calculation for the decay rate is applicable in this case. This method complements the estimates for the thermal dispersion around equilibrium discussed in Section 4.1, with the important difference that the sub-critical bubble calculations do include the non-linearities in the problem, being by definition non-perturbative.

The free energy of a spherically symmetric fluctuation around equilibrium is

$$F(T) = 4\pi \int_0^\infty r^2 dr \left[\frac{1}{2} \left(\frac{d\phi}{dr} \right)^2 + V_{\text{EW}}(\phi, T) \right]. \quad (4.9)$$

We will focus on the electroweak model at T_C . In principle, there will be fluctuations from $\phi = 0$ to ϕ_+ and back, although at T_C the free energies for these fluctuations are identical. The rates for the thermal fluctuations can be estimated by making an ansatz

for the radial profile of the sub-critical bubbles. Following Ref. 22 we write

$$\phi_+(r) = \phi_+ \exp(-r^2/\ell^2), \quad (4.10)$$

where $\phi_+(r)$ corresponds to a bubble of broken phase ϕ_+ nucleated in the symmetric phase $\phi = 0$. The parameter ℓ controls the approximate size of the bubble which we take to be the correlation length. Introducing the dimensionless variables $X(\rho) = \phi(r)/\sigma$, $\tilde{\ell}(T) = \ell(T)\sigma$, $\theta = T/\sigma$, and $\rho = r\sigma$, we obtain

$$F_+(\theta) = \pi^{3/2} X_+^2 \tilde{\ell} \sigma \left[\frac{3\sqrt{2}}{8} + \tilde{\ell}^2 \left(\frac{D\sqrt{2}}{4} (\theta_C^2 - \theta^2) - \frac{E\theta_C\sqrt{3}}{9} X_+ + \frac{\lambda_T}{32} X_+^2 \right) \right]. \quad (4.11)$$

In Fig. 8 we show $F_+(T_C)/T_C$ as a function of the Higgs mass and the top mass. In order for sub-critical bubbles to be of cosmological relevance, their thermal nucleation rate must be considerably larger than the expansion rate of the Universe, $\Gamma(\xi(T), T)/H > 1$, with $H \simeq 1.66 g_*^{1/2} T^2/M_{\text{PL}}$, where $g_* \simeq 110$ is the number of effective relativistic degrees of freedom at the electroweak scale. Neglecting pre-factors, this condition can be easily seen to lead to the inequality $F_+(T)/T < 34$. From Fig. 8 it is clear that at T_C this condition is comfortably satisfied for the present lower bound on the Higgs mass, $M_H \geq 57$ GeV, for which we obtain $\Gamma(\xi, T_C)/H \sim 10^8$.

Recently, Dine *et al.* argued that sub-critical bubbles would not be of relevance for most (if not all) the parameter space of the standard model due to the smallness of the thermal dispersions around $\langle \phi \rangle = 0$.⁸ We agree with their results for $M_H \sim 60$ GeV. However, for larger Higgs masses fluctuations in long wavelengths are quite large, contrary to their claim. We hoped to have shown here that both the estimate from the thermal dispersion and from sub-critical bubbles indicate that there will be large fluctuations around equilibrium, signaling the failure of the 1-loop potential to describe the dynamics of the transition.

V. CONCLUSION

In this work we have argued that it is possible to study the critical behavior of a weak first order transition which has a spinodal instability at some temperature T_2 by mapping its behavior around equilibrium, $\langle\phi\rangle$, to an effective Ginzburg-Landau model above its critical temperature T_2 . In this way, both models have the same spinodal instability at $\langle\phi\rangle$ so that infrared corrections can be estimated from well-known ε -expansion methods. This approach is completely general and can in principle be applied to any sufficiently weak first order transition. It suits the standard electroweak model particularly well due to the closeness of its critical temperature T_C to the spinodal instability temperature T_2 . In fact, the difference between the two temperatures should provide a qualitative measure of the weakness of the transition.

Incorporating the ε -expansion results leads to a larger correlation in the spatial fluctuations of the order parameter, which can be translated into a smaller (infrared corrected) mass for excitations around $\langle\phi\rangle$. Thus, the strength of the transition is considerably weaker than one would estimate from the naïve 1-loop potential. We do not claim here to have obtained the ε -corrected effective potential, but an estimate of the infrared corrections which are not included in the 1-loop result. Our results provide a simple way to examine the importance of these corrections around T_C , offering a simple way of estimating the strength of the transition. If the η parameter is close to unity at the critical temperature T_C the transition is well described by the 1-loop result. Otherwise, the transition is weakly first order, and one should be very careful when adopting the usual vacuum decay formalism to study the transition. As a pictorial representation of the complexity of the behavior of a weakly first order transition, we show in Fig. 3 the behavior of a ϕ^4 model around T_C . For clarity, we show only the black and white values of ϕ , defined to be for $\phi < 0$ and $\phi \geq 0$, respectively. The critical behavior of the system

is then in the same equivalence class as the 2-dimensional Ising model. This simulation is done by starting the system at $\phi = +\phi_0$ and $T = 0$, and by studying the temperature behavior of the system by immersing it in a thermal bath at temperature T .¹⁵ For temperatures just below or above T_C , the large fluctuations around equilibrium are quite apparent. In particular, one can picture the behavior of this system just below its critical temperature as being qualitatively similar to the behavior of a weak first-order transition at its critical temperature.

We have also discussed two other simple ways of estimating the strength of the transition based on the thermal dispersion around equilibrium and on the sub-critical bubbles method. When applied to the 1-loop electroweak potential both approaches suggest that there will be large fluctuations around equilibrium, indicating that the 1-loop result does not fully describe the dynamics of the transition. In fact, the results here show that the actual dynamics of the transition may be much more complex than the usual scenario based on vacuum decay calculations.

ACKNOWLEDGEMENTS

We would like to thank F. Alcarraz, R. Holman, J. Langer, and S. Shenker for important discussions. We also thank the hospitality of the Institute for Theoretical Physics at Santa Barbara where this work was developed during the Cosmological Phase Transitions workshop. This work was partly supported in Santa Barbara by the National Science Foundation under Grant No. PHY89-04035. EWK was partly supported by NASA under Grant NAGW-2381 at Fermilab and by the DOE at Chicago and Fermilab.

References

1. V. A. Kuzmin, V. A. Rubakov, and M. E. Shaposhnikov, *Phys. Lett.* **155B**, 36 (1985).
2. M. E. Shaposhnikov, *Nucl. Phys.* **B287**, 757 (1987); P. Arnold and L. McLerran, *Phys. Rev. D* **36**, 581 (1987); M. Dine, O. Lechtenfeld, B. Sakita, W. Fischler, and J. Polchinski, *Nucl. Phys.* **B342**, 381 (1990); N. Turok and J. Zadrozny, *Phys. Rev. Lett.* **65**, 2331 (1990); *Nucl. Phys.* **B358**, 471 (1991); A. G. Cohen, D. B. Kaplan, and A. E. Nelson, *Phys. Lett.* **245B** (1990) 561; *Nucl. Phys.* **B349**, 727 (1991); M. Dine, P. Huet, R. S. Singleton Jr., and L. Susskind, *Phys. Lett.* **257B**, 351 (1991).
3. A. G. Cohen, D. B. Kaplan, and A. E. Nelson, in Ref. 2.
4. N. Turok and J. Zadrozny, in Ref. 2.
5. L. Dolan and R. Jackiw, *Phys. Rev. D* **9**, 3320 (1974); S. Weinberg, *ibid.*, 3357 (1974).
6. G. W. Anderson and L. J. Hall, *Phys. Rev. D* **45**, 2685 (1992); M. Dine, P. Huet, and R. Singleton, *Nucl. Phys.* **B375**, 625 (1992).
7. D. Brahm and S. D. H. Hsu, Caltech preprints, CALT-68-1705 and CALT-68-1762 (1991); M. E. Shaposhnikov, *Phys. Lett.* **B277**, 324 (1992); M. E. Carrington, *Phys. Rev. D* **45**, 2933 (1992).
8. M. Dine, R. Leigh, P. Huet, A. Linde, and D. Linde, *Phys. Rev. D* **46**, 550 (1992).
9. P. Arnold, University of Washington preprint UW/PT-92-06 (1992).
10. P. G. De Gennes, *The Physics of Liquid Crystals*, (Clarendon, Oxford, [First edition, reprinted 1975]).

11. L. A. Fernández, J. J. Ruiz-Lorenzo, M. Lombardo, and A. Tarancón, *Phys. Lett.* **B277**, 485 (1992).
12. See, for example, K. G. Wilson and J. Kogut, *Phys. Rep.* **12C**, 75 (1974).
13. P. Ginsparg, *Nucl. Phys.* **B170**[FS1], 388 (1980).
14. E. Brézin, in *Methods in Field Theory*, Les Houches 1975, Session XXVIII, ed. R. Balian and J. Zinn-Justin, (North-Holland, Amsterdam 1976).
15. F. F. Abraham, M. G. Alford, and M. Gleiser, *in progress*.
16. M. Gleiser, *Phys. Rev. D* **42**, 3350 (1990).
17. M. Gleiser, E. W. Kolb, and R. Watkins, *Nucl. Phys.* **B364**, 411 (1991).
18. N. Tetradis, DESY preprint DESY 91-151 (1991).
19. C. Itzykson and C. B. Zuber, *Quantum Field Theory*, (McGraw-Hill, New York, 1980).
20. E. W. Kolb and Y. Wang, *Phys. Rev. D* **45**, 4421 (1992).
21. L. D. Landau and E. M. Lifshitz, *Statistical Physics*, 3rd ed. (Pergamon, New York, 1980), Pt. I.
22. M. Gleiser and E. W. Kolb, Fermilab preprint FERMILAB-PUB-91/305-A (1991), *in press Phys. Rev. Lett.*
23. D. A. Huse and D. S. Fisher, *Phys. Rev.* **B35**, 6841 (1987); C. Tang, H. Nakanishi, and J. S. Langer, *Phys. Rev.* **A40**, 995 (1989).
24. A. M. Srivastava, University of Minnesota preprint, TPI-MINN-91/37-T (1991).
25. G. B. Gelmini and M. Gleiser, *in progress*.

Figure Captions

FIG. 1. The 1-loop electroweak potential at several different temperatures.

FIG. 2. The parameter $x = E^2/\lambda_T D$ as a function of the Higgs mass for several values of the top quark mass.

FIG. 3. 2-dimensional simulation of ϕ^4 model for different temperatures. Initial conditions were chosen such that at $t = 0$ the field is in the equilibrium state $\phi = +\phi_0$, given by the G-L model at $T = 0$.

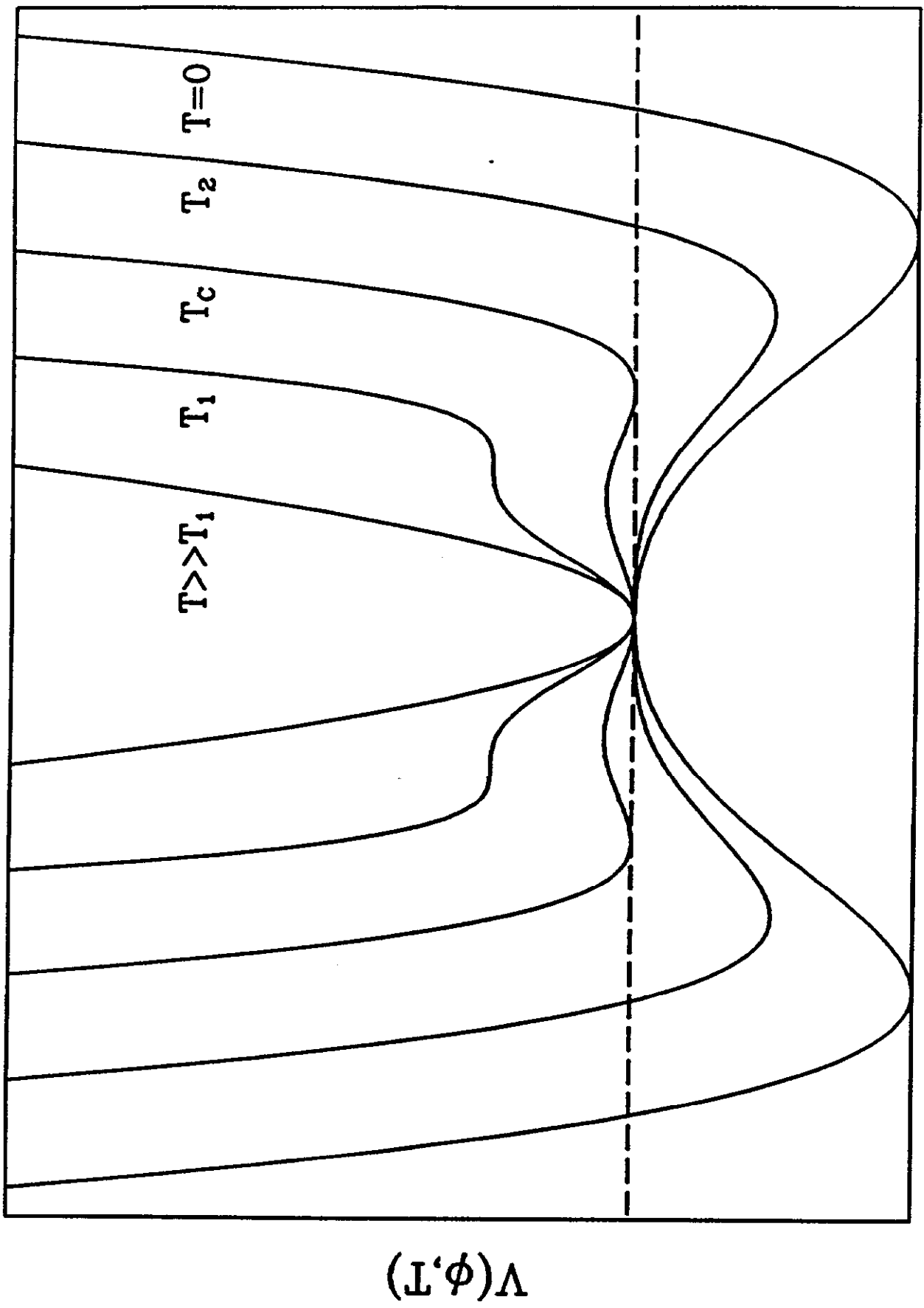
FIG. 4. The 1-loop electroweak potential (solid curves) and the associated G-L model of Section 3.1 (dashed curves) for temperatures T_C (a) and T_2 (b). A Higgs mass of 100 GeV and a top quark mass of 130 GeV were chosen.

FIG. 5. The ε -corrected mass as a function of the Higgs mass for several values of the top mass.

FIG. 6. The G-L model obtained by neglecting the left-right symmetry in the electroweak model and by transforming away its cubic term.

FIG. 7. The ratio $\phi_{int}^2/2\Delta(\xi)$ as a function of the Higgs mass for $M_T = 130$ GeV at T_C .

FIG. 8. The free energy of the sub-critical fluctuation at the critical temperature as a function of the Higgs mass for several values of the top quark mass.



ϕ

FIG. 1 Gleiser & Kolb

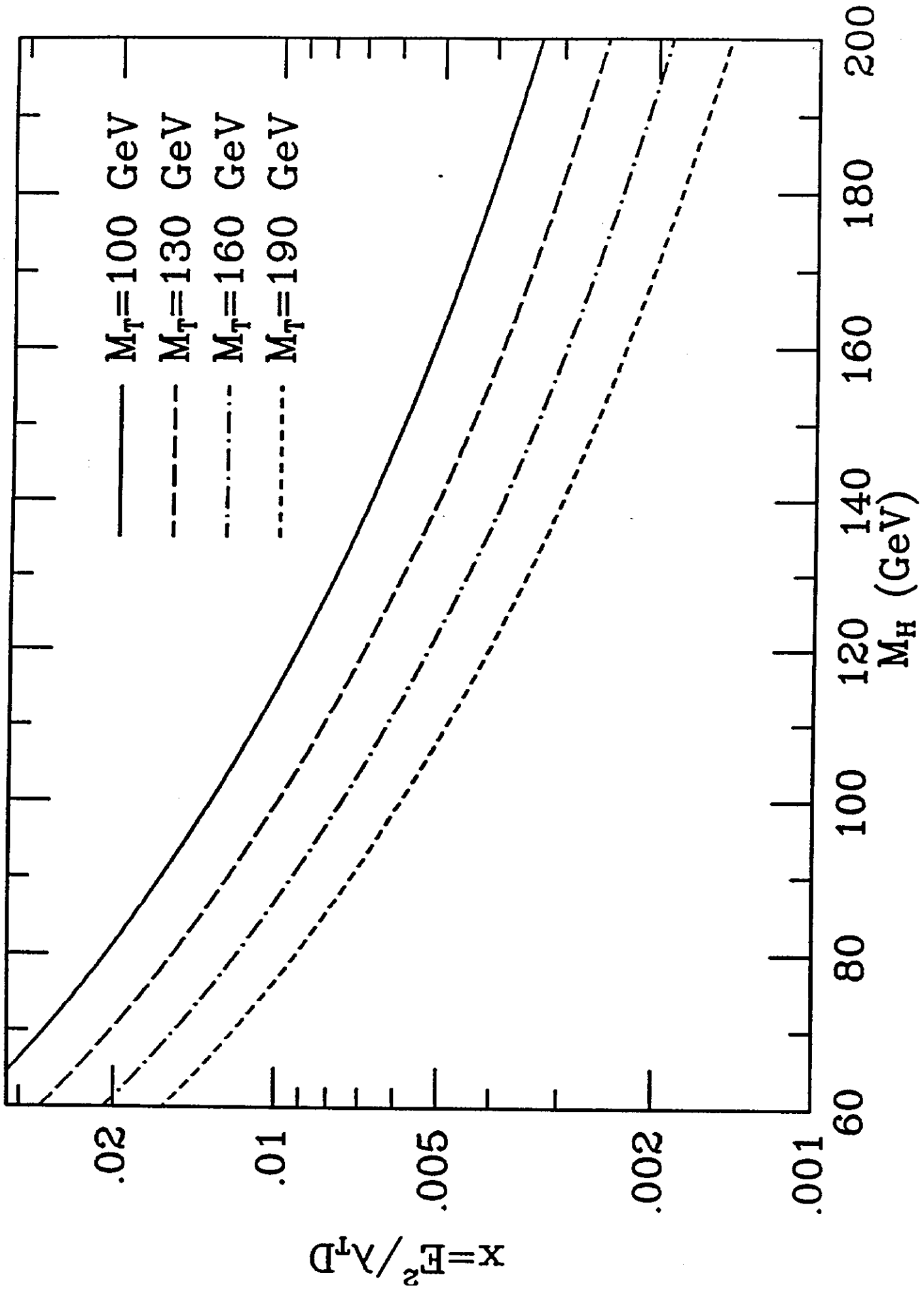
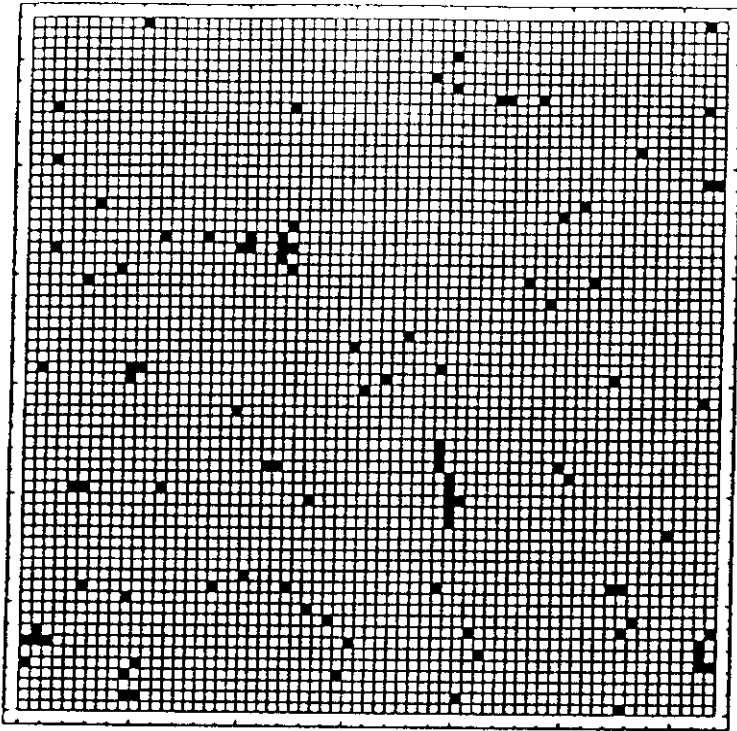
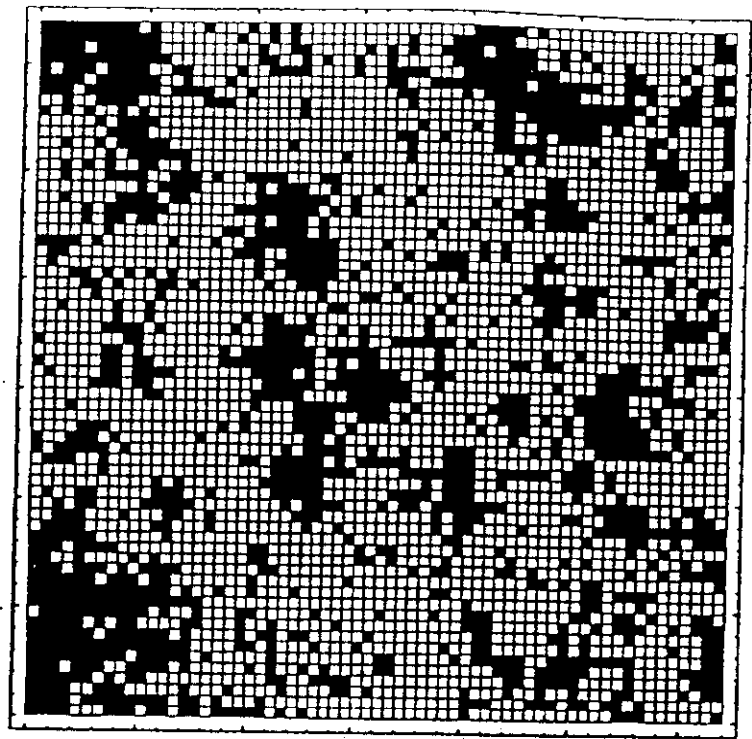


FIG. 2 Gleiser & Kolb

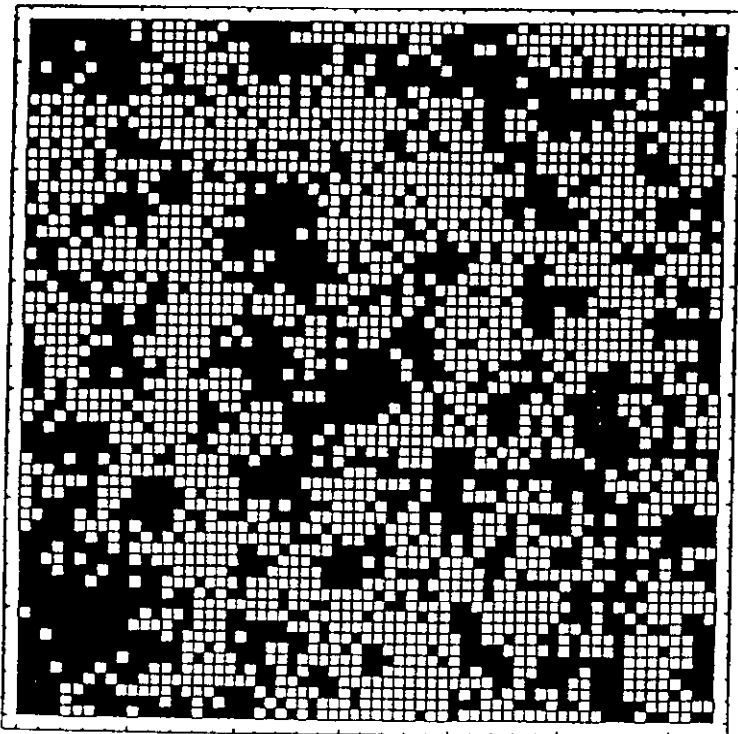
a) $T < T_c$



b) $T \lesssim T_c$



c) $T \gtrsim T_c$



d) $T \gg T_c$

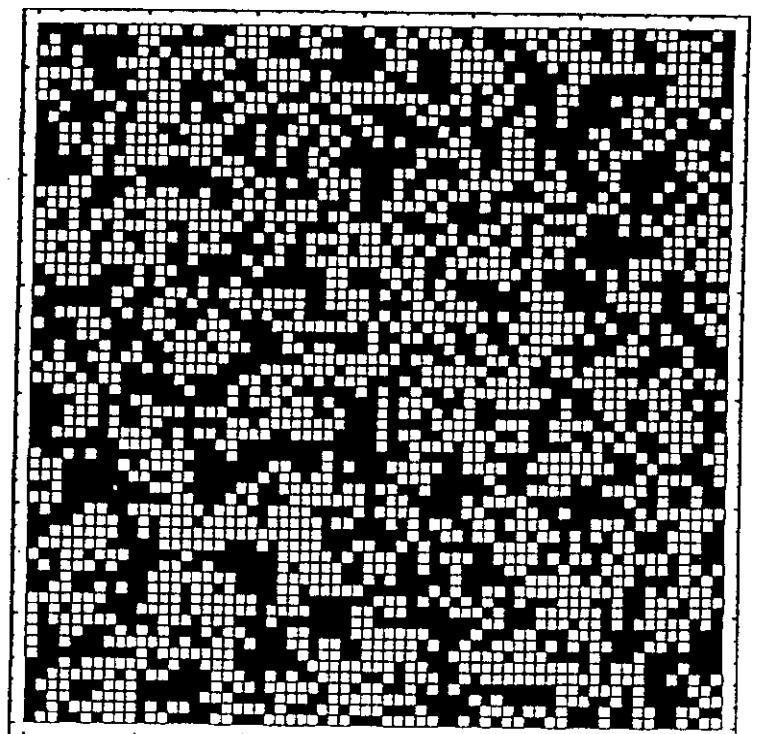


FIG. 3 Gleiser & Kolb

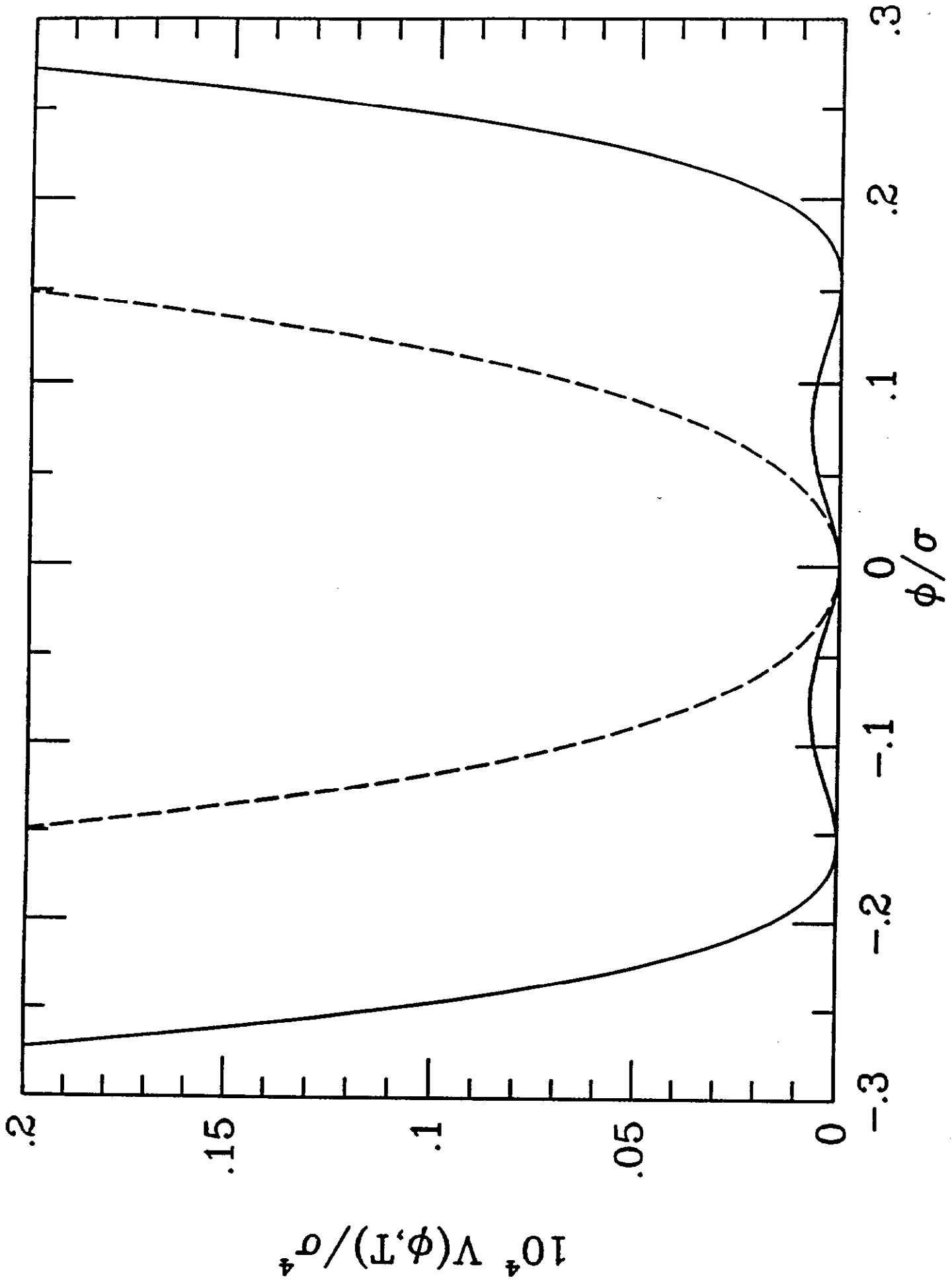


FIG. 4a Gleiser & Kolb

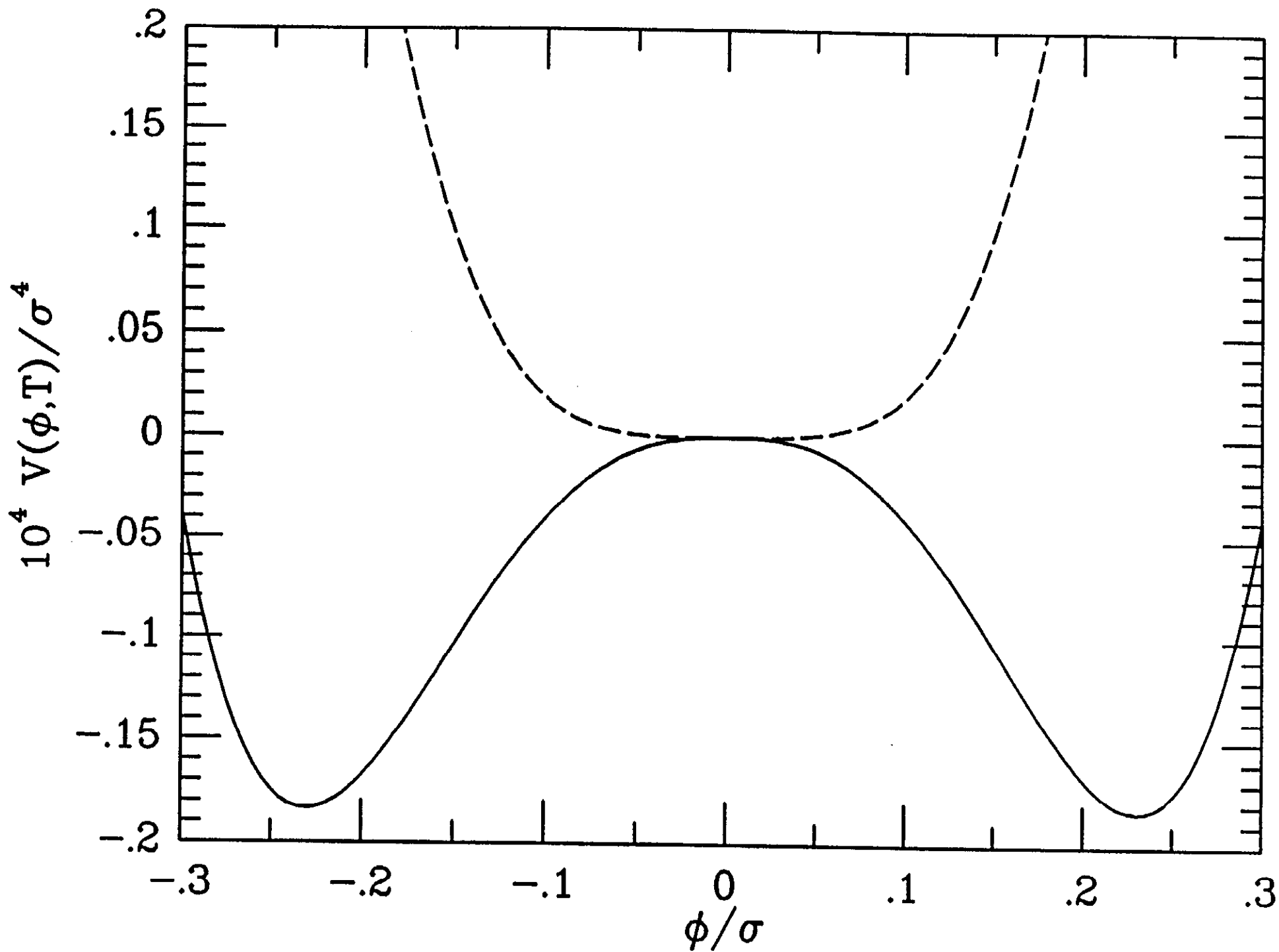


FIG. 4b Gleiser & Kolb

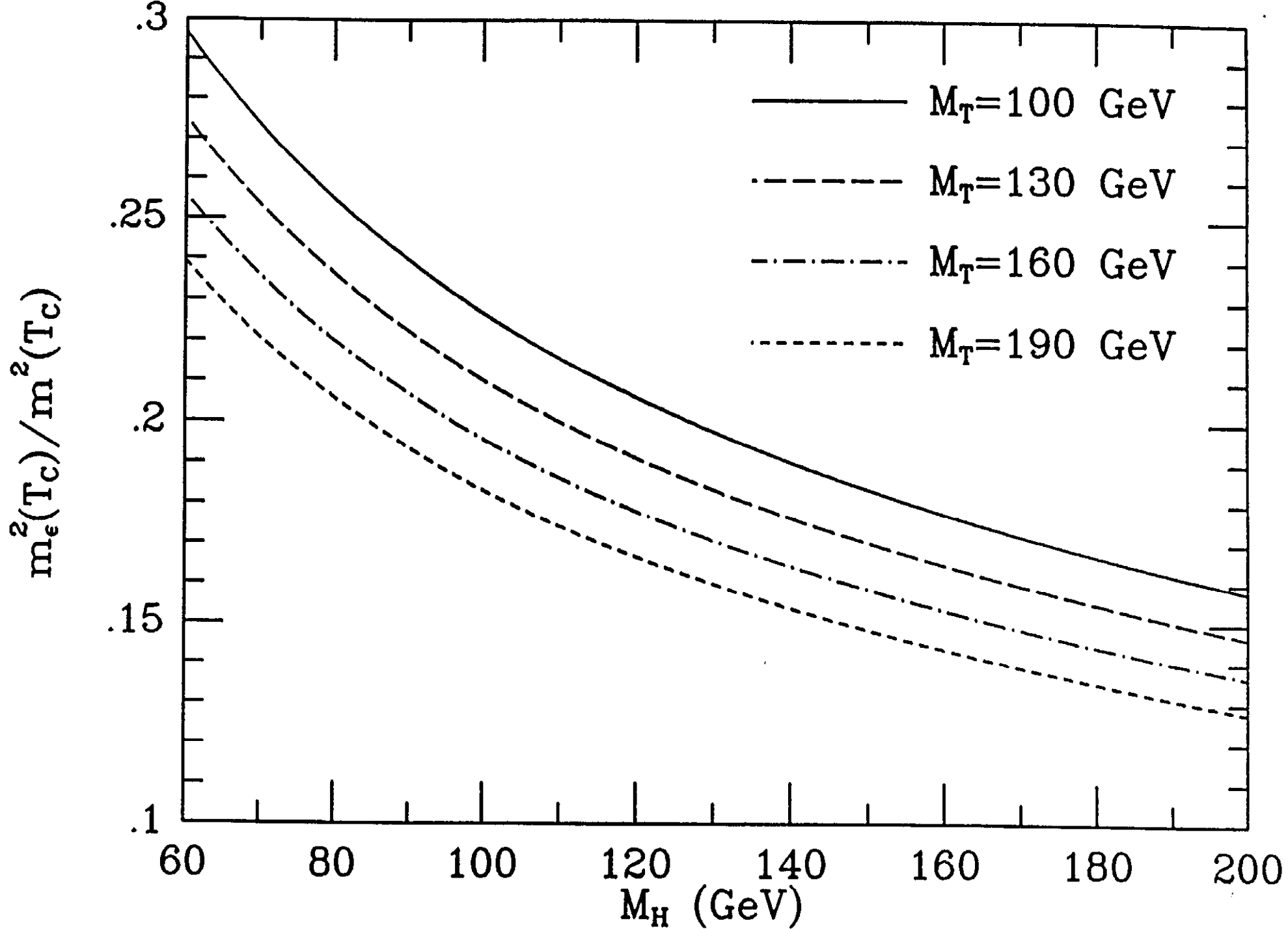


FIG. 5 Gleiser & Kolb

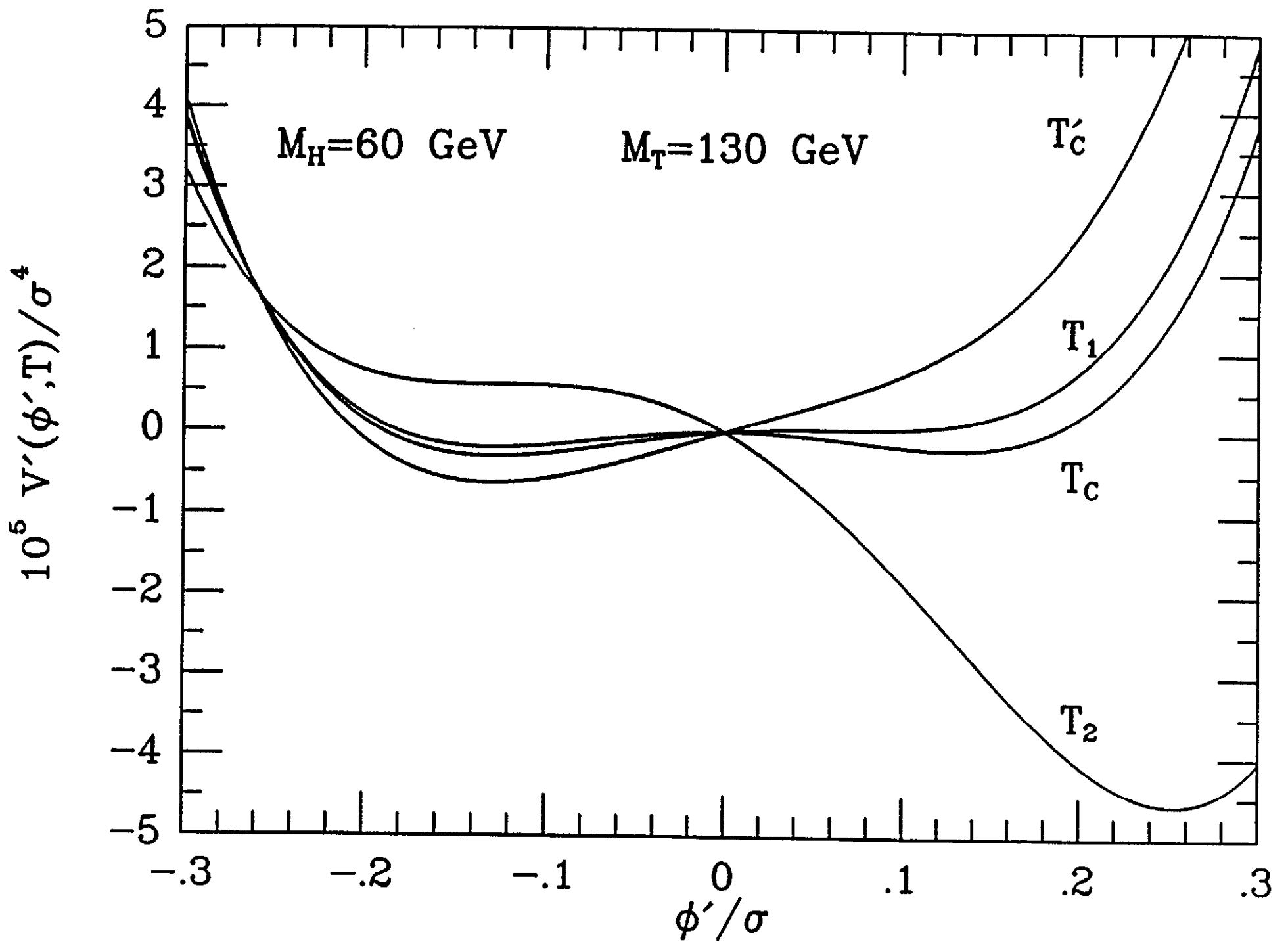


FIG. 6 Gleiser & Kolb

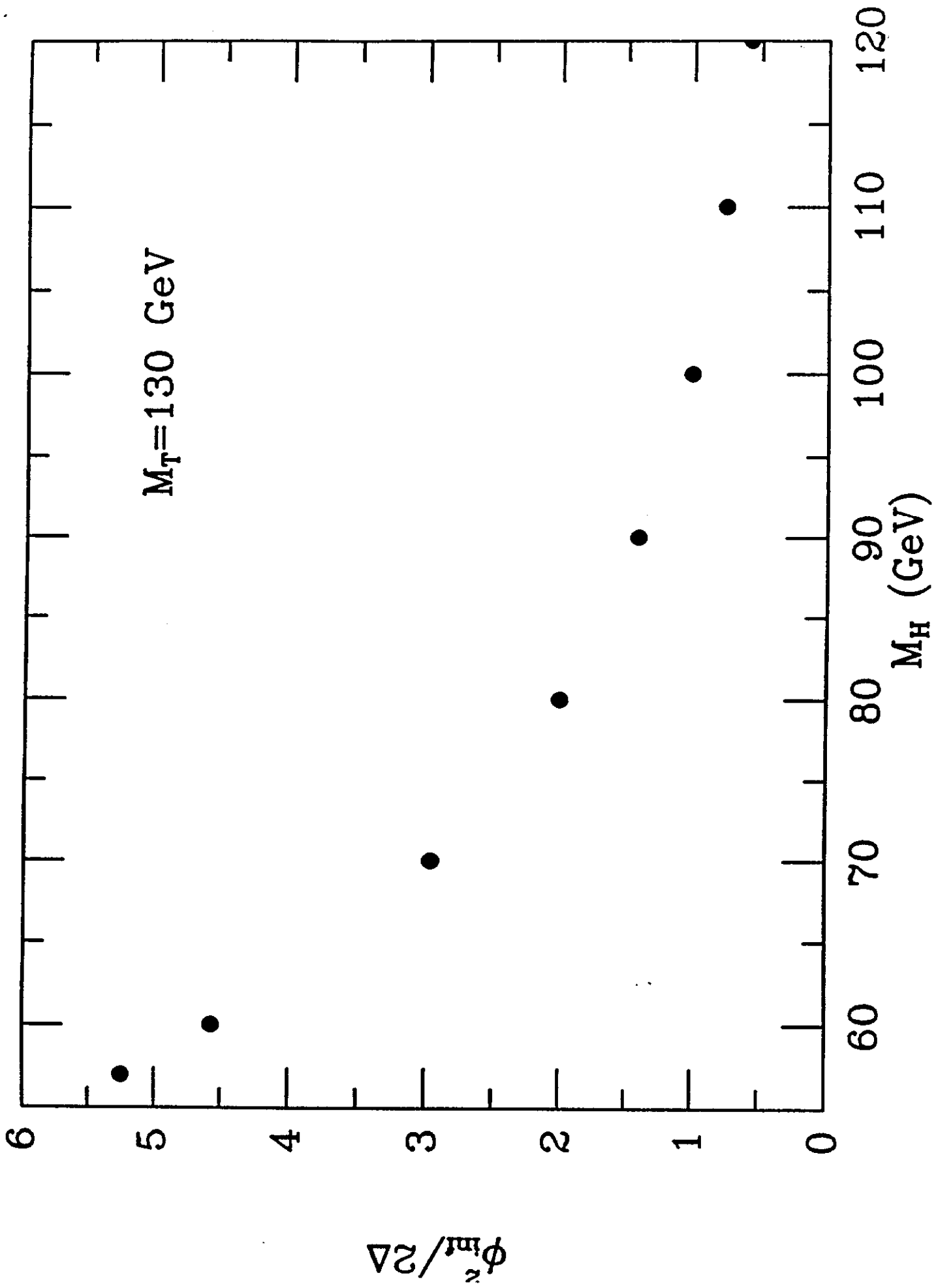


FIG. 7 Gleiser & Kolb

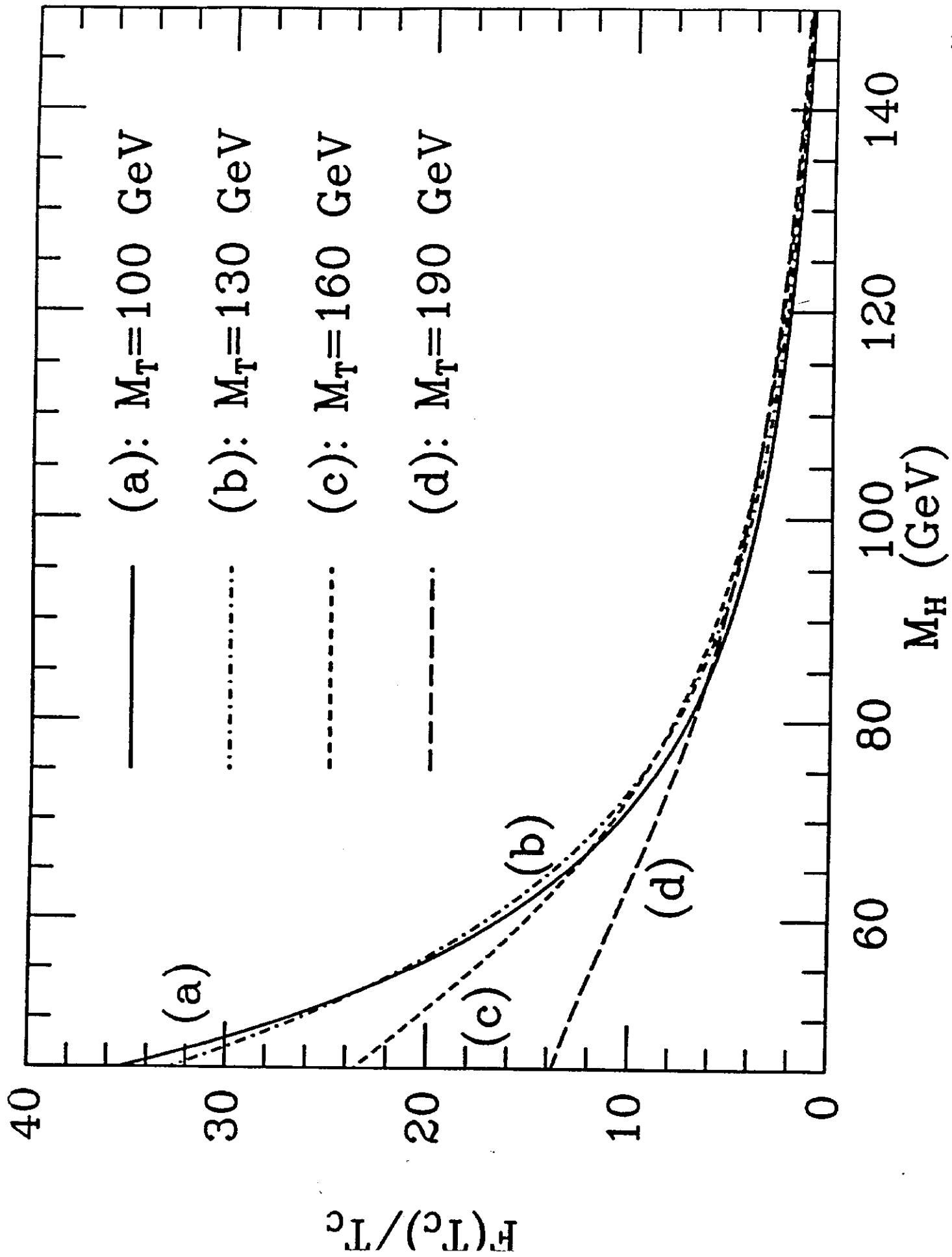


FIG. 8 Gleiser & Kolb